STEPHY Publishers

Trends in Petroleum Engineering

Research Article

ISSN: 2771-2494

Experimental Research on Bit Side Force and Anti-deviation in Vertical Well

Zhang H[1,2]*

[1]State Key Laboratory of Shale Oil and Gas Enrichment Mechanisms and Effective Development, Beijing, China

[2]Sinopec research institute of petroleum engineering, Beijing 102206, China

Abstract

Based on dimensional method, the similarity criterion of simulation test was derived. The experimental apparatus was established in accordance with the similarity criterion. A series of experiments with different drilling parameter were carried out. The experimental results show that with rotary speed rise, the bit side force fluctuation increased, however, the vibration energy at the dominant frequency decreased, at low rotary speed, the dominant frequency of the bit side force is equal to rotation frequency of drill string, and at high rotary speed, the dominant frequency is consistent with the backward whirl frequency of drill string, which is about 3 times of rotation frequency, moreover, as WOB rise, the vibration energy at dominant frequency increased, while the total wave energy decreased, and the critical rotary speed value at the jump process of the dominant frequency increased. Furthermore, for the purpose of deviation controlled straight drilling, there is the problem of optimization grouping between WOB and rotary speed.

Keywords: Bit side force,Well deflection drill string vibration, Experiment

Introduction

Well deflection is a crucial indicator to evaluate the hole quality in drilling, and bit side force is a key parameter judging the inclination control effect in the technique of inclination control. Therefore, many of scientists and engineers in the field of drilling have done the massive theoretical research work for bit side force and have established a number of mathematics calculation models. The certain result obtained from the theoretical researches was applied for field,[1-4] however it is inaccurate to analyse side force at bit only through the theoretical analysis. With the development of down-hole logging while drilling technology and indoor measurement technology, some progress is made on the research of bit side force by analysing down-hole measured field data and conducting laboratory simulation experiments. In order to measure the bit side force during drilling,[5,6] Millheim[7], Maron[8] and others designed a short section of the test structure which can measure the axial force, bending moment and shear force for derivation of the bit side force. However, the high cost of measurements and the complex working conditions on site are resulting in the incomplete measured data. So in this paper, the laboratory simulation test has become an important mean to research the bit side force. To establish lab simulation test device, this paper derived the simulation test of similarity criterion by using dimensional analysis method. According to the principle of similitude, an experimental device for investigating the bit side force was designed and set up. And a series of experiments with different drilling parameter was carried out to study the influencing factor on the bit side force during vertical rotary drilling.

Quick Response Code:

***Corresponding author:** Hongning Zhang, No.5 Baisha Road, Changping District, Beijing, China

Received: 18 May, 2022 **Published:** 13 June, 2022

Citation: Zhang H. Experimental Research on Bit Side Force and Anti-deviation in Vertical Well. *Trends Petro Eng*. 2022;2(1):1–8. DOI: 10.53902/TPE.2022.02.000514

Deduction of Similarity Criterion

There are three main methods to deduce the similarity criterion such as law of deduction, equation derivation method and dimensional method. The dimensional method is commonly used for designing dynamic test device, so this method was used to deduce the simulation test of similarity criterion in this paper.[9-11]To better analyse dimension, treating the bottom hole assembly as a shaft with uniformly-distributed mass, and discounting for the impact of drill string eccentricity and drilling fluid damping. The parameters and their dimension in this experiment are shown in table 1.

Table 1: Drill string dynamics model parameters and dimensions.

Physical quantity	Symbol	Dimension
outer diameter of drill string	D	L
internal diameter of drill string	d	
length of drill string	l	
hole diameter	D_h	
gyration radius of drill string	r	
lateral displacement	x,y,z	
elastic Modulus	E	$ML^{-1}T^{-2}$
mass of drill string	m	M
weight on bit(WOB)	w	MLT^{-2}
friction force on side-wall	f	
weight of drill string	G	
density of drill string	ρ	ML^{-3}
inertia torque of section	I	L^4
rotation speed	R	T^{-1}
angle of deviation	α	$L^0M^0T^0$
elastic rigidity	N	MT^{-2}

To facilitate the dimensional analysis, the parameters in table 1 which have the same dimension were replaced by the same symbol in derivation. For example, the outer and internal diameter, length, gyration radius of drill string, hole diameter and lateral displacement have the same dimension, so letter 'l' can be used to represent them. Similarly, 'F' can be used to represent the WOB, friction force on well wall, and weight of drill string. Angle α is dimensionless, so which can be neglected in derivation. Therefore, there are only eight parameters with different dimension in coefficient matrix, the dimension of the parameters was shown in table 2.

Table 2: Coefficient matrix.

Basic dimension	L	E	ρ	m	I	F	R	N
M	0	1	1	1	0	1	0	1
L	1	1	-3	0	4	1	0	0
T	0	2	0	0	0	-2	-1	-2

Because of the rank of the coefficient matrix r is 3, the dimensionless deposition of the matrix is 5. A non-singular matrix could be composed by the three basic physical quantities of l, E, ρ, so which were selected as basic physical quantities. It's important to note that, in in the derivation, the any three physical quantities in table 1 which could be composed of nonlinear matrix can be used as the basic physical quantities. There is no effect on the result of the derivation. Any other physical quantity with the three basic physical quantities could form dimensionless value. As an example, a dimensionless value was composed with the physical quantity m and the three basic physical quantities, and the solution process of the coefficient is as follows.

The dimensionless quantity can be written as:

$$\pi_1 = \rho^{k_1} l^{k_2} E^{k_3} m \tag{1}$$

Where π_1 is dimensionless physical quantity, m is a physical quantity in coefficient matrix.

Because π_1 is dimensionless, the simultaneous equations can be given by:

$$\left.\begin{aligned} k_1 + 0 + k_3 + 1 &= 0 \\ -3k_1 + k_2 + k_3 &= 0 \\ 0 + 0 + 2k_3 &= 0 \end{aligned}\right\} \tag{2}$$

After solution of the equation 2, where k_1 is -1, $k_2$is -3, and k_3 is 0, so the π_1 can be expressed as $\rho^{-1}l^{-3}m$. Similarly, the other physical quantity can be expressed by the three basic physical quantities as follows.

$$\left.\begin{aligned} \pi_1 &= \rho^{-1}l^{-3}m = \frac{m}{\rho l^3} \\ \pi_2 &= l^{-4}I = \frac{I}{l^4} \\ \pi_3 &= l^{-2}E^{-1}F = \frac{F}{l^2E} \\ \pi_4 &= \rho^{\frac{1}{2}}l^1E^{-\frac{1}{2}}R = Rl\sqrt{\frac{\rho}{E}} \\ \pi_5 &= \rho^1 l^2 l^3 N = \frac{F}{lE} \end{aligned}\right\} \tag{3}$$

Because the dimensionless physical quantity of the prototype in Eq. 3 equal to the model, the Eq. 4 to the Eq. 8 can be deduced. In the follow equations, the letters with subscript 'm' represents model parameter and the letters with subscript 'p' represents prototype parameter. The relationship between prototype and model can be expressed as follows:

$$\left(\frac{m}{\rho l^3}\right)_m = \left(\frac{m}{\rho l^3}\right)_p ;\ m_p = \frac{{l_p}^3\rho_p}{{l_m}^3\rho_m} m_m = {c_l}^3 c_\rho m_m \tag{4}$$

$$\left(\frac{I}{l^4}\right)_m = \left(\frac{I}{l^4}\right)_p ;\ I_p = \frac{{l_p}^4}{{l_m}^4} I_m = {c_l}^4 I_m \tag{5}$$

$$\left(\frac{F}{l^2E}\right)_m = \left(\frac{F}{l^2E}\right)_p ;\ F_p = \frac{{l_p}^2E_p}{{l_m}^2E_m} F_m = {c_l}^2 c_E F_m \tag{6}$$

$$\left(Rl\sqrt{\frac{\rho}{E}}\right)_m = \left(Rl\sqrt{\frac{\rho}{E}}\right)_p;$$

$$R_p = \frac{l_p}{l_m}\sqrt{\frac{\rho_p E_m}{\rho_m E_p}}R_m = c_l c_\rho^{\frac{1}{2}} c_E^{-\frac{1}{2}} R_m \quad (7)$$

$$\left(\frac{N}{lE}\right)_m = \left(\frac{N}{lE}\right)_p;\ N_p = \frac{l_p \rho_p}{l_m \rho_m}N_m = c_l c_E N_m \quad (8)$$

From the above equations, the similarity relationship of the parameters between the prototype and the model can be shown as:

$$\begin{cases} c_l = \frac{l_p}{l_m} c_l = \frac{l_p}{l_m} c_E = \frac{E_p}{E_m} c_F = \frac{F_p}{F_m} \\ c_m = \frac{m_p}{m_m} c_R = \frac{R_p}{R_m} c_\rho = \frac{\rho_p}{\rho_m} c_N = \frac{N_p}{N_m} \end{cases} \quad (9)$$

If the proportional relationship of the parameters between the experiment and filed satisfy the Eq. (4)-(9), the phenomena observed in experiment was almost similar to actual drilling filed.

Experimental Equipment

Based on similarity criterion, the testing apparatus was established in accordance with the proportion of 1:10 between the test model and field prototype.[12-18] As shown in Figure 1 and Figure 2, the total height of the testing apparatus is 15m, which include simulated wellbores, simulated drill pipe, measuring system and processing program software. The height of the simulated wellbores is 13m with different sizes of inner diameter of 24mm, 32mm and 44mm. In order to ensure similar elasticity modulus between the simulated wellbore and the actual borehole wall, the organic glass was selected to make simulated wellbores with 3.8MPa elasticity modulus. The simulated drilling string was installed within the simulated wellbore, the height of which is nearly 14m and there are also three kinds of outer diameter of 16mm, 18mm and 22mm. The simulated drill pipe was made with ABS plastics which has the similar stress-strain characteristics to the actual drill pipe. The measuring system comprises pressure sensors, lateral force sensor, displacement sensor, electromechanical amplifier and acquisition collector. The pressure sensors and the lateral force sensors were installed in the bottom of the testing apparatus to measure the pressure and lateral force of the bit. The processing program software was used to process the collected data and draw the bit side force curve of the bit in real-time.

The loop force-measuring ring is shown in Figure 3, which circumferential contact with the simulation bit. Three pressure sensors are evenly distributed along the ring numbered selectively as 1#, 2# and 3#. During simulation rotary-percussive drilling process, the loop force-measuring ring could measure the force that caused by instantaneous impact of the simulation bit.

In experiment, the forces measured by the three pressure sensors are respectively corresponding to the F_1, F_2 and F_3 in figure 3.

The N_b is the resultant force of F_1, $F_2$and F_3, which is named the bit side force. For convenience of analysis, the resultant force is divided into *x*-axis component force and the *y*-axis component force of N_{bx} and N_{by}. The conversion relationship between the resultant force and the component force can be expressed as follows:

$$\begin{cases} N_b = \frac{1}{2}\sqrt{3(F_3 - F_2)^2 + (2F_1 - F_2 - F_3)^2} \\ N_{bx} = \frac{\sqrt{3}}{2}(F_3 - F_2) \\ N_{by} = F_3 - \frac{1}{2}(F_2 + F_3) \end{cases} \quad (10)$$

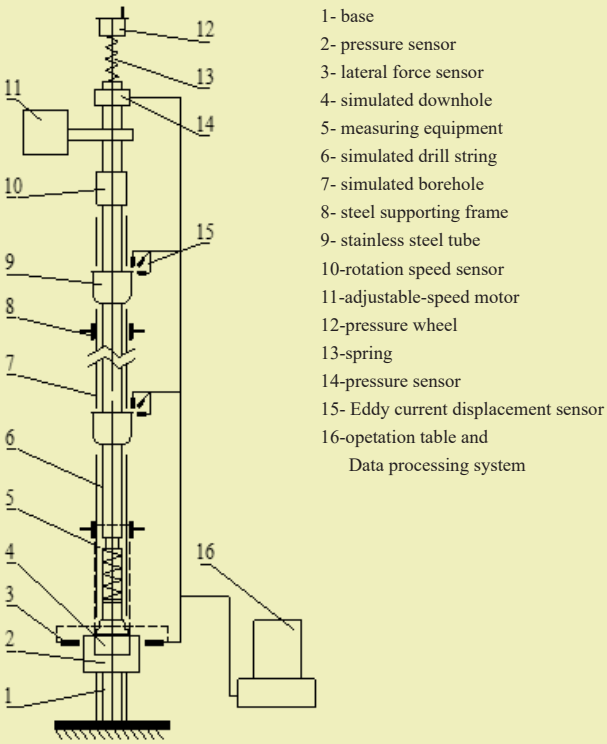

Figure 1: Structure chart of testing apparatus

Figure 2: Photo of testing apparatus

After the geometry of the test apparatus is determined, the WOB and rotate speed are important optional test parameters. When the test rotate speed is 2.796 times of the actual speed and

the test WOB is 1/9130 times of actual WOB, the simulated drill pipe has similar motion to the actual drilling filed. The proportion relationship between the test and the actual working conditions is shown in Table 3 and Table 4.

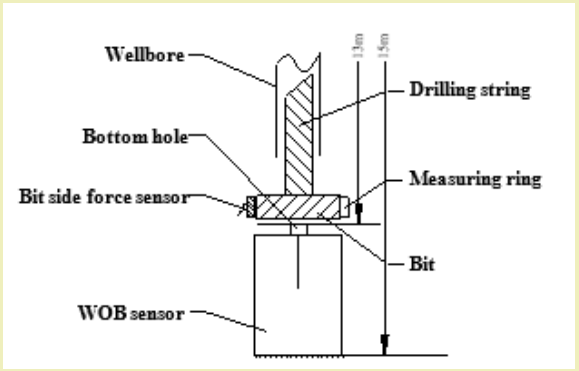

Figure 3: Measuring device of the bit side force

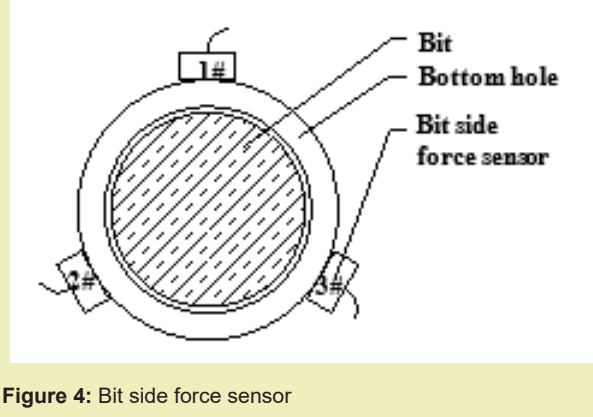

Figure 4: Bit side force sensor

Table 3: Corresponding Relationship of rotational speedbetween model and prototype.

Test Number	*R1*	*R2*	*R3*	*R4*	*R5*	*R6*
rotational speed of model/(r/min)	70	120	170	220	270	320
rotational speed of prototype /(r/min)	25	43	61	79	97	115

Table 4: Corresponding Relationship of WOB between model and prototype.

Test Number	*w1*	*w2*	*w3*	*w4*	*w5*
WOB of model /kg	0.5	1	1.5	2	2.5
WOB of prototype /KN	45	90	134	179	223

There are two kinds of the bottom hole assembly (BHA) prototype to simulate in experiment, one is Φ215.9 mm PDC bit + Φ159 mm collar×2 + Φ214 mm helical centralizer + Φ159 mm collar×22 + Φ127 mm drill pipe, the other isΦ311 mm PDC bit + Φ228 mm collar×2 + Φ310 mm helical centralizer + Φ228 mm collar×22 + Φ127 mm drill pipe. The two kinds of BHA are pendulum drill assembly which was the common and effective BHA used in field.

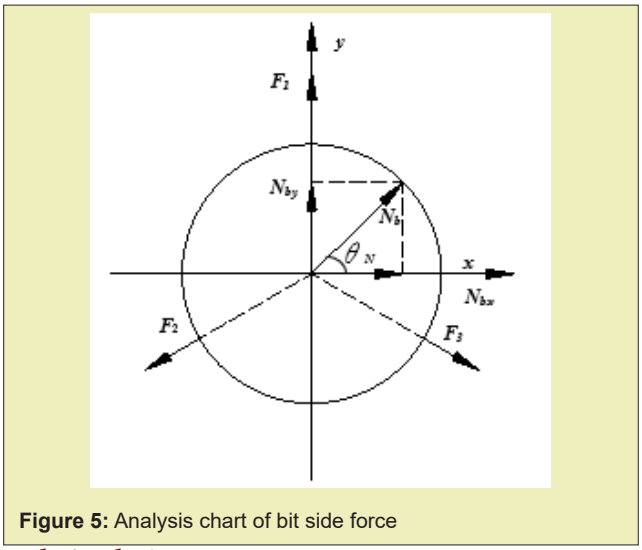

Figure 5: Analysis chart of bit side force

Result Analysis

Influence of rotation speed

Through the Eq. 10, the bit side force N_b can be divided into deflecting force N_{bx} and azimuth force N_{by}. Under different drilling parameters conditions, the time-domain plots of N_{bx} and N_{by} are shown in Figure 6, and the frequency range charts of N_{bx} and N_{by} are shown in Figure 7. In the top of the Figure 6 and the Figure 7, the letter *N* represents rotary speed and the letter *W* stands for WOB. In Fig. 6 the black thin lines reflect measured value and the red heavy lines stand for mean value. In Figure 6 and Figure 7, the transverse three pictures are in the condition of the same rotary speed, from left to right of the pictures the weight on bit is, in order, 0.5 kilogram, 1.5 kilogram and 2.5 kilogram. The longitudinal three pictures are in the condition of the same weight, from top to bottom of the pictures the rotary speed is, in order, 120r/min, 220r/min and 320r/min.

From these figures, the changing rules of fluctuation range of the bit side force can be observed. In the condition of the identical WOB, at low rotary speed, the fluctuation signals of the azimuth force N_{by} has obvious periodicity, and the symmetry about the *x* axis of the measuring data of the azimuth force is poor; At high rotary speed, the periodicity of the azimuth force is not so significant, and the symmetry of the measuring data is better. The different symmetry about the *x* axis in the different speed conditions results the sum of the bit side force in the fixed time is large at low speed, and the sum is small at high speed. And with rotary speed increasing, the bit side force fluctuation increased, the fluctuation of the azimuth force increased from 8N at low speed to 40N at high speed.

From Figure 7, the frequency and the changing rules of wave energy of the bit side force can be analysed. As rotary speed rise, the total wave energy of the bit side force increased, however, the vibration energy at the dominant frequency decreased (the dominant frequency means a specific frequency in which the wave energy is

maximal). The frequency of the bit side force is closely related to rotation frequency of drill string, at low rotary speed, the dominant frequency of the bit side force is equal to rotation frequency of drill string; at high rotary speed, the dominant frequency is consistent with the backward whirl frequency of drill string, which is about 3 times of rotation frequency. There is a critical rotary speed value from the dominant frequency equal to 1 time of rotation frequency to the dominant frequency equal to 3 times of rotation frequency.[19]

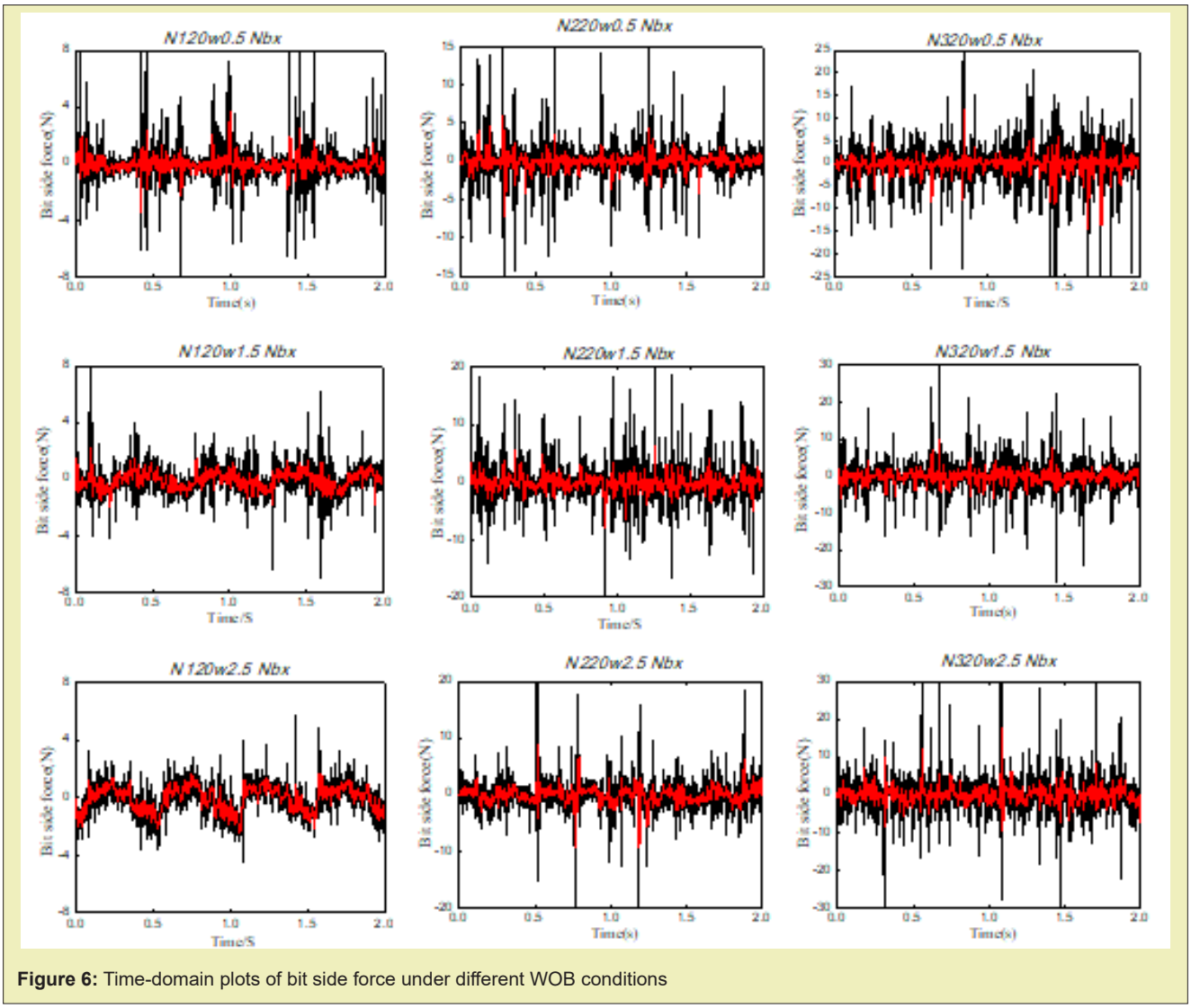

Figure 6: Time-domain plots of bit side force under different WOB conditions

Because there is no component of gravity in peripheral direction of the borehole, the change rule of the deflecting force N_{bx} along with the change of rotating speed is basically identical to the azimuth force N_{by}, just the fluctuation range of N_{bx} is slightly higher than N_{by}. Therefore, this paper only analyse the influence factors of N_{bx}.

Influence of WOB

In the condition of the same rotary speed, at low WOB, the periodicity of the azimuth force is not so significant, and the symmetry about the *x* axis of the azimuth force N_{by} is good; At high WOB, the azimuth force N_{by} has obvious periodicity, and the symmetry about the *x* axis is poor. Because of the different symmetry about the *x* axis in the different WOB conditions, the sum of the bit side force in the fixed time is small at low WOB, and is big at high WOB. With WOB increasing, the bit side force fluctuation increased.

From Figure 7, the frequency and the changing rules of wave energy of the bit side force can be analysed. As WOB rise, the vibration energy at dominant frequency increased, while the total wave energy decreased. And the critical rotary speed increased. For instance, the critical rotary speed is 170r/min at the weight is 0.5kg, however, when the weight is 2.5kg, the rotary speed value is nearly 330r/min. The rule of the bit side force variation with the drilling parameters is similar with the rule of drilling string lateral vibration.

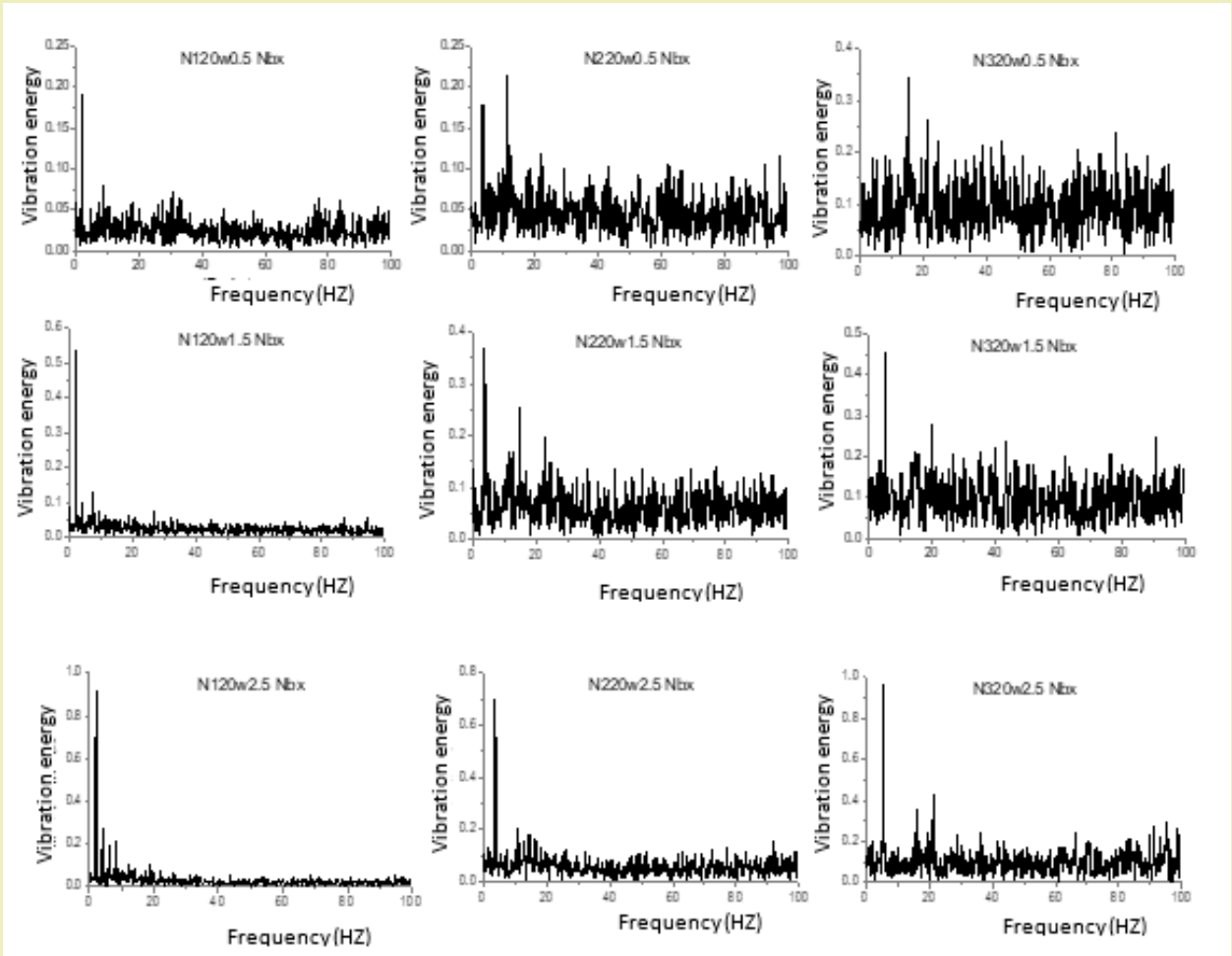

Figure 7: Frequency range charts of bit side force under different WOB conditions

Distribution rule of bit side force

In order to visually analyse the influence of drilling parameters on the bit side force, the arithmetic mean value of the bit side force in the *X* direction and the *Y* direction were calculated respectively in 5 seconds and a period of drill string rotation. By studying the arithmetic mean value, the influence factors of the bit side force was analysed. The Figure 8 illustrates the changing rule of the average value of the bit side force under different drilling parameter. In this figure, the solid lines represent the arithmetic mean value of the bit side force in 5seconds, and the dashed lines indicate the arithmetic mean value of the bit side force in a period of drill string rotation. The Figure 9 reflects the distribution of the bit side force in coordinate axis under the condition of different WOB, and the Figure 10 reflects the distribution under the condition of different rotation speed. In Figure 8 and Figure 9, the value of these points corresponds to *X*-axis is equal to N_{bx}, and which corresponds to Y-axis is equal to N_{by}.

From Figure 8, the bit side force increases as WOB becomes bigger, and with the increase of speed, the bit side force increases at first, and then decreases, when speed is up to 170r / min, the maximum bit side force appears. Moreover, the arithmetic mean value of the bit side force in 5seconds is almost identical to which in a period of drill string rotation, which means the measuring data in fixed times is reliable.

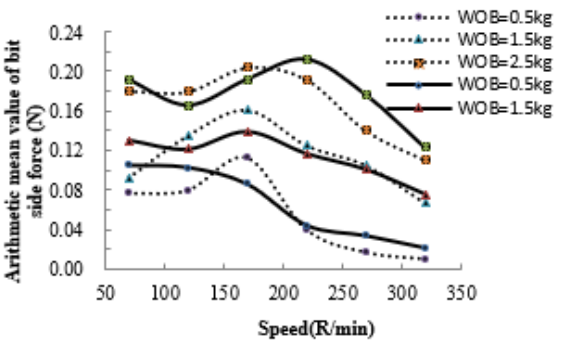

Figure 8: Arithmetic mean value of the bit side force variation with drilling parameters

From Figure 9 and Figure 10, an obvious random feature can be found on the distribution of the bit side force in each quadrant of coordinate system. However, with the increase of WOB, the position of the bit side force in coordinate system gradually spread to the periphery, and as the speed increase, the position of the bit side force in coordinate system gradually close to the origin.

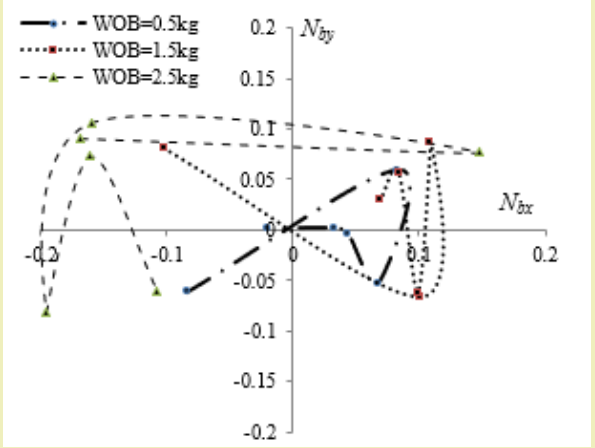

Figure 9: Distribution of bit side force under different WOB conditions

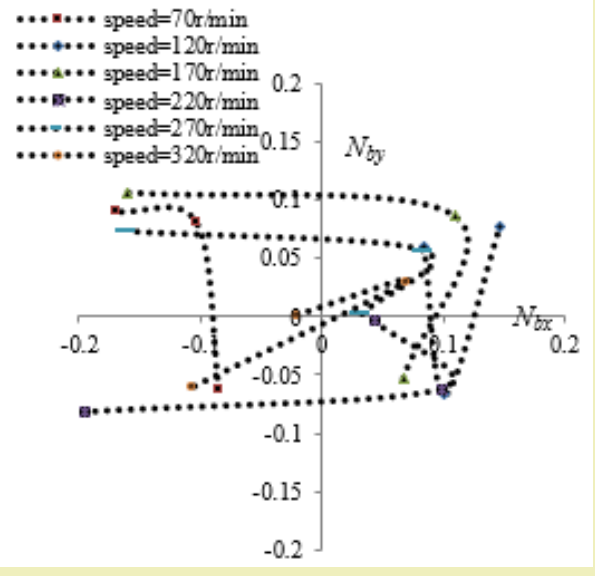

Figure 10: Distribution of bit side force under different speed conditions

Therefore, for the purpose of deviation controlled straight drilling, it should keep the rotate speed from 170 r/min in engineering practice, because at this point the bit side force is maximal. Furthermore, in drill operation, drilling with high rotate speed and low WOB has certain inclining prevention function, because the bit side force is minimal in the drilling parameters.

Conclusion

Based on dimensional method, the similarity criterion of simulation test was derived, and the experimental apparatus was established in accordance with the similarity criterion. Moreover, a series of experiments with different drilling parameter was carried out, which can reflect dynamic change of the bit side force under different conditions.

As rotary speed rise, the bit side force fluctuation increased, however, the vibration energy at the dominant frequency decreased. At low rotary speed, the dominant frequency of the bit side force is equal to rotation frequency of drill string, and at high rotary speed, the dominant frequency is consistent with the backward whirl frequency of drill string, which is about 3 times of rotation frequency. As WOB rise, the vibration energy at dominant frequency increased, while the total wave energy decreased. And the critical rotary speed value increased.

In drill operation, drilling with high rate of revolution and low WOB has certain inclining prevention function, and keep the speed value from 170r/min is beneficial to drilling.

Acknowledgements

The support of the National Science and Technology Major Project (2011ZX05021-001) and National Key Basic Research and Development Program (973 Program), China (2010CB226706) are gratefully acknowledged.

Funding

None.

Conflicts of Interest

Author declares that there is no conflict of interest.

References

1. Knight MJ. Brennan FP. Dover WD. Fatigue Life Improvement of Threaded Connect ions by Cold Rolling. Journal of Strain Analysis for Engineering Design. *Journal of Strain Analysis for Engineering Design.* 2005;40(2):83–93.
2. Chen DCK. Integrated BHA Modeling Delivers Optimal BHA Design. Middle East Drilling Technology Conference. Doha. 2007; pp. 41–51.
3. Neubert M. Heisig G, Forstner I. Verification of an Advanced Analysis Mo del with Downhole Bending Moment Measurements. Asia Pacific Oil & Gas Conference. Kuala Lumpur, 2005, pp. 793–802.
4. Chen DCK, Comeaux B. Real time Downhole Torsional Vibration Monitor for Improving Tool Performance and Bit Design. Drilling Conference, Kuala Lumpur, 2006; pp. 1189–1197.
5. Chen DCK, Smith M, LaPier re S. Advanced Drill string Dynamics System Integ rates Real– time Modeling and Measurement. Latin American and Caribbean Petroleum Engineering Conference. Rio de Janeiro, 2003, pp. 645–656.
6. Zhi BJ, Nao SY. The Theory and Practice of Hole Control. Beijing: Petroleum Industry Press. 1990.
7. Millheim KK. System for measuring downhole drilling forces. U. S. Patent 4445578, 1984.

8. Maron R. Apparatus for measuring weight-torque and side force on a drill bit. U. S. Patent 4958517,1990.

9. Cai SY, Yan Y, Fan WC. Setting up a simulate device on motion behavior of bottom–hole assembly according to similitude principles. Journal of Guangxi University: Natural Science Edition. 2006;17(1):159–162.

10. Jie YJ. Similitude Principle and Structure Model Experimental. Wuhan: Wuhan University of Technology Press. 2005.

11. Min ZZ. Zhen Zhemin Collected Works. Beijing: Science Press. 2003.

12. Gen CT, Chuan GZ. Drilling engineering theory and technology. Dongying: China University of Petroleum Press. 2006.

13. Chuan GZ, Cai SY, Yan X. Research on motion state of bottom hole assembly and the evaluation method of drilling tendency. Petroleum Drilling Techniques. 2005;33(1):24–27.

14. Zhong WW, Chuan GZ, Wang LY. Experimental study on longitudinal vibration characteristics of pendulum assembly in straight hole. *Journal of China University of Petroleum: Edition of Natural Science.* 2007;31(1):64–68.

15. Macpherson JD, Jogi PN, Kingman JEE. Application and analysis of simultaneous near bit and surface dynamic measurements. *SPE Drilling and Completion.* 2001;12(1):230–238.

16. Zhong WW, Chuan GZ, Wang LY. Correlation experimental study on weight on bit (WOB) fluctuation characteristics of pendulum assembly and unbalanced assembly. *Journal of Oil and Gas Technology.* 2008;30(1):157–160.

17. Cheng L, Huai DT, Peng W. Measurement method and experimental research on dynamic force behavior of bottom drill string. *Chinese Journal of Mechanical Engineering.* 2009;20(1):933–936.

18. Tao FY, Li GD, Jun F. Research on the simulation test method for dynamic properties of BHA. *Chinese petroleum machinery.* 2012;41(1):6–10.

19. Chuan GZ, Fa WY, Xin JY. Experimental research on motion behavior of bottom drill string in straight hole. *Acta PetroleiSinica.* 2003;24(3):102–106.